İSTİFLEME AÇISININ FİBER TAKVİYELİ KOMPOZİT PLAKALARDA ÇARPILMAYA ETKİSİ

Kenan ÇINAR[1]

Özet

Fiber takviyeli kompozit malzemeler pişirme süreci sonrasında kalıptan ayrıldığında tasarlandığı şekilden farklı bir şekil almaktadır. Üreticilerin kullandığı deneme yanılma yöntemleri ile toleranslar içerisinde kompozit parçalar üretilmekte fakat bu yöntem pahalı ve zaman alıcıdır. Bu problemin çözümü mutlak şekil değişimini tahmin etmek ve sonra istenilen son şekil değişimini veren kalıbı tasarlamaktır. Bundan dolayı düz parçaların üretim sırasında çarpılmasını ön gören 3 boyutlu bir sonlu elemanlar modeli geliştirilmiştir. Bunun yanında istiflenme açısının çarpılmaya etkisi incelenmiştir.

Anahtar Kelimeler: Sonlu elemanlar yöntemi, kompozit malzemeler, süreç modellenmesi, artık gerilmeler.

EFFECT OF STACKING SEQUENCE ON THE WARPAGE OF FIBER REINFORCED COMPOSITE PLATES

Abstract

A fibre reinforced composite part generally takes a different shape from the one that is originally designed after removing from the mould at the end of the curing process. Traditional method used by manufacturers is a trial and error approach to fabricate the composite parts within the dimensional tolerances but this method is very expensive and time consuming. The solution of this problem is to predict the absolute magnitude of the distortion and then to design a mould that gives the desirable final shape according to the prediction. Thus a 3D Finite Element (FE) model was developed to predict the warpage values occur during manufacturing of flat laminates. In addition, the effect of stacking sequence on warpage was investigated.

Keywords: Finite element method, composite materials, process modeling, residual stresses.

[1] Araş. Gör. Dr, Namık Kemal Üniversitesi, kcinar@nku.edu.tr

Introduction

Fibre reinforced composite materials have been increasingly used in various structural components in aerospace, marine, automotive and wind energy sectors. Although manufacturing and investment costs of composite materials are high as compared to conventional materials, primarily metals, their higher strength per unit weight, less machining and fastening operations increase the popularity of composite materials day by day. The direction dependent mechanical properties of composite materials can also be advantageous in some applications where strength is only required in a specific direction.

In aerospace applications, fibre reinforced composite materials are manufactured by autoclave processing in order to achieve low void content (<0.1%) required for aerospace components. In the autoclave manufacturing technique, resin pre-impregnated layers of fibres called prepregs are sequentially laid on the mould in predetermined stacking sequence, covered with a peel ply, breather and vacuum bag in order.

During the process pressure and heat are applied according to the process curing cycle. A different Manufacturer Recommended Cure Cycle (MRCC) is used for each prepreg systems because each prepreg system has different resin chemistry. The aim of the cure cycle is to cure the resin with low void content and bond the resin to the fibres.

In the processing of composite materials, generally the final shape of the composite parts is not the same as the mould shape after the process. Also, process induced distortions cannot be entirely eliminated. In the literature these distortions are represented by spring-in in curved parts and by warpage in flat parts. A reduction in enclosed angles of a curved region is called spring-in. Problems occur during and after the assembly of parts due to poor contact between mating surfaces unless the magnitude of these distortions are predicted within the tolerances. The solution of this problem is very complex because the absolute magnitude of the distortion is difficult to predict and is often variable in production even the production conditions held constant. In manufacturing floor, a trial and error approach is preferred to solve these problems but this method is very expensive and time consuming in manufacturing of large components. If the distortions are predicted closely in advance the investment to the trial and error modification can be prevented. The basic reason behind the distortion is the process induced residual stresses occurring during the manufacturing process. The unbalanced distribution of residual stresses inside the composite materials results in deformation, matrix cracking, and even delamination. In the literature five main mechanisms or sources have been identified responsible for process induced residual stresses; mismatch in the thermal expansion coefficients, resin cure shrinkage, tool-part interaction, cure gradients and volume fraction gradients.

White and Hahn (White and Hahn, 1992) developed a process model which predicts a residual stress history during the curing of composite materials by including the effects of chemical and thermal strains. The mechanical properties of composite materials depend on the degree of the cure state of the composite materials. They used Bogetti and Gillespie's (Bogetti and Gillespie, 1992) cure kinetics model in their study in order to find the degree of cure at the any moment during the cure cycle. The relation

between the degree of cure and mechanical properties is modelled by a power law equation. In their elastic residual stress model, laminated plate theory was used and for viscoelastic residual stress model, the quasi elastic method was used. They combined the cure kinetics and viscoelastic stress analysis to calculate residual moment and in turn find the curvatures simultaneously. In their model, unsymmetrical cross-ply flat laminates were used only. The model did not include the tool-part interaction.

(Johnston et al., 2001) developed a plane strain finite element model which employs a Cure Hardening, Instantaneous Linear Elastic Constitutive (CHILE) model to predict process-induced stress and distortion of composite laminates. They analysed the effect of thermal expansion, cure shrinkage, temperature gradients, degree of cure, resin flow and mechanical constraints on the deformation of the laminates. The tool-part interaction was modelled by elastic "shear layer", which performed until the tool is removed. Their predicted and measured spring-in values were correlated for $[0]_{24}$ lay-up; however the correlation was bad for $[90]_{24}$.

(Svanberg and Holmberg, 2001,2004 and Svanberget et al.,2005) developed a simplified mechanical constitutive model to predict the shape distortions. They assumed that the mechanical behaviour of the material is constant within rubbery and glassy states and there is a step change in the properties at the glass transition temperature. The rubbery properties they used were simply assumed to be about two orders of magnitude smaller than those in the glassy state. They used three different tool-part interaction models in their FE analysis; freestanding, fully constrained, and frictionless contact conditions. The predictions indicated that the contact boundary conditions give the closest agreement to the measured spring–in. Then they used their finite element model to predict the spring-in in brackets produced by Resin Transfer Moulding. There were no experimental data about the rubbery properties and the tool-part interaction was oversimplified, which were the main drawbacks of their numerical analysis. Comparison between experimental and predicted shape deformations indicate that after the second cure step the predicted spring-in shows good agreement with the experimental values but after the third cure step the prediction is poor. Their predictions overestimate the spring-in angle after the third cure step.

(Ersoy et al., 2010) developed a two-step 2-D finite element model including anisotropy in the thermal expansion coefficient and cure shrinkage to predict the process induced stress and deformation. The two-step model was representing the rubbery and glassy states of the resin. The reason for preferring two-step approach was the complexity of the determining continuous development of material properties during cure schedule. In each step constant material properties were used. Gelation occurs at approximately 30 % degree of cure, and vitrification occurs at approximately 70 % degree of cure for the resin. Gelation and vitrification are considered to be two main transitions during the curing process. Ersoy used these transitions between the steps of his model. In the first step of the model, before vitrification, rubbery material properties were used, whereas in the second step, after vitrification, glassy material properties were used. The development of resin properties at the rubbery state were predicted by using Group Interaction Modelling (GIM) and then the mechanical properties of the composite were predicted through the two different micromechanics methods, namely Self Consistent Field Micromechanics (SCFM) and Finite Element Based Micromechanics (FEBM). The properties of the composite at the glassy state were

determined by both experimentally and numerically. The predictions for the glassy properties were very close to experimental values (Ersoy et al., 2010). In this study, a part geometry and tool material is chosen to minimise the issues related to tool–part interaction and consolidation and hence, the stresses developed before gelation is ignored. Spring-in values predicted by the two-step FEA are very close to the measurements for both unidirectional and cross-ply C-shaped composite parts. The predictions follow the trend of decreasing spring-in with increasing thickness, which matches well with experimental results. The measured spring-in angles are very close to predicted ones for the thicker parts, and slightly lower for the thinner parts, with a maximum difference of 15 %. Wisnom et al. explained the phenomenon of decreasing spring-in with increasing thickness by some shear deformation (shear-lag) between plies to maintain the same arc length during curing, which in turn decreases the amount of in-plane stress and causes smaller spring-in values(Wisnom et al., 2007).

The first objective of this study is to investigate the effect of stacking sequence on the warpage of the flat laminates. The second objective of this study is to develop three dimensional FE model to predict the process induced deformations for an autoclave processing of composite flat laminates by taking into account the interactions in early stages of cure. The predictions of shape distortions of parts obtained by the process models are then compared to the distortions measured by 3d laser scanning.

Experimental work

Materials and Manufacturing

The 4 plies of flat laminates with the dimension of 300x50 mm were manufactured by using an autoclave. The autoclave has a inner diameter of 1200 mm and a working length of 1500 mm. (Figure 1) shows a flat composite laminate prepared within a vacuum bag on the flat tool plate prior to curing.
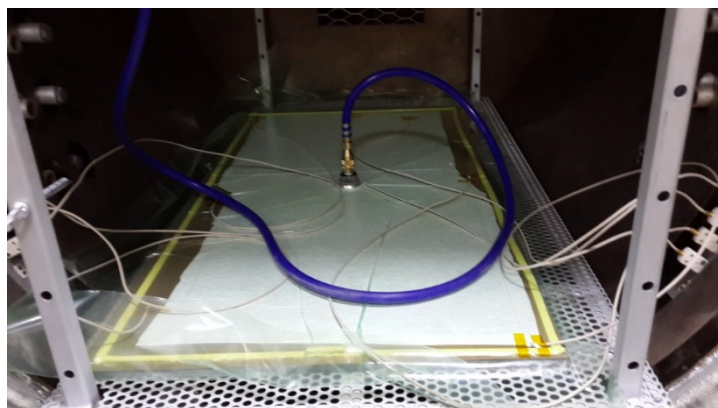

Figure 1. Flat composite plate bagged up on a steel tool inside the autoclave.

The magnitude of warpage was compared by changing the stacking sequence of the samples. The stacking sequence of the manufactured strips are given in (Figure 2). The length and the width of the strips are 300 mm and 50 mm respectively, as shown in

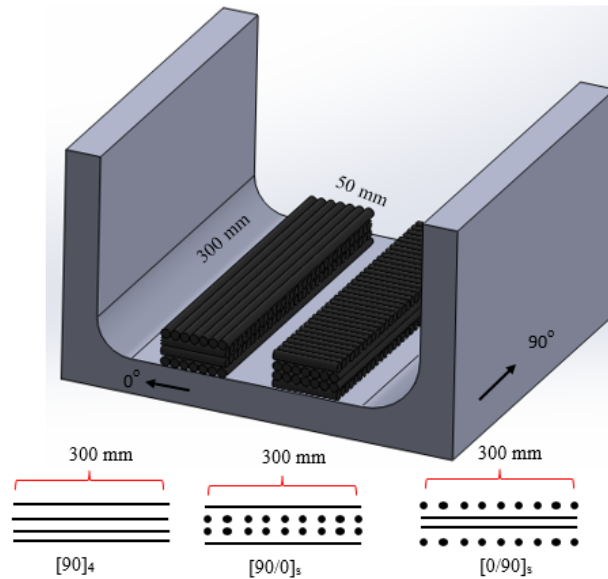(Figure 2). The stacking sequence of the UD samples are $[90]_4$ and XP samples are $[90/0]_s$ and $[0/90]_s$.

Figure 2. Schematic representation of strip placement and stacking configuration.

Materials Used

The material used was a unidirectional carbon-epoxy prepreg material produced by Hexcel Composites with a designation of AS4/8552. The nominal thickness of the single prepreg was specified to be 0.184 mm and the nominal fibre volume fraction as 57.4%. The physical properties of the prepreg used are given in (Table 1).

Table 1. Physical properties of AS4/8552

	Value	Units
Fibre Density	1.79	g/cm^3
Resin Density	1.30	g/cm^3
Nominal Cured Ply Thickness	0.184	mm
Nominal Fibre Volume	57.42	%
Nominal Laminate Density	1.58	g/cm^3

The manufacturer's Recommended Cure Cycle (MRCC) includes five steps. In the first step, the part is heated up to 120°C at 2°C/min. In the second step, it is held at 120°C for 60 minutes. In the following step, it is heated up from 120°C to 180°C at 2°C/min. Then, the part is held at 180°C for 120 minutes. Finally, the part is left to cool down to room temperature before removal from the mould. 0.7 MPa pressure is applied

from the beginning to the end of the process and vacuum is applied up to the middle of the second step.

Measurement of Part Geometry

The parts manufactured were scanned by a METRIS MCA II 7- axis laser scanner in order to capture the full deformation pattern of the parts. The scanned geometry of the part in the form of a point cloud was virtually placed on the nominal tool through three edge points and the gap distances between the tool and the part are found using a commercial software.

Numerical Method

The three-step 3-D finite element model including anisotropy, cure shrinkage, consolidation, and tool-part interaction was developed to simulate the process-induced distortion.

Steps of Analysis

The resin states with respect to the MRCC is shown in (Figure 3a) together with the glass transition temperature and degree of cure of the resin. The gel point which is defined as the point where the prepreg is cured enough to sustain in-plane shear stresses, and the vitrification point at which the instantaneous glass transition temperature reaches the process temperature are also indicated. The resin is believed to be gelled at around 160 $^{\circ}$C during the second ramp as a sharp rise of the glass transition temperature. The vitrification where the glass transition temperature reaches the process temperature occurs 45 minutes after the 180 $^{\circ}$C soak period starts [75]. The steps of the FE model are shown in (Figure 3 b). The whole cure stage was divided into three distinct regions according to resin modulus development during curing. Actually resin in the viscous form does not sustain any mechanical loads but the entangled fibres within the resin can bear some mechanical load in the viscous state so that linear elastic behaviour is assumed in the viscous step.
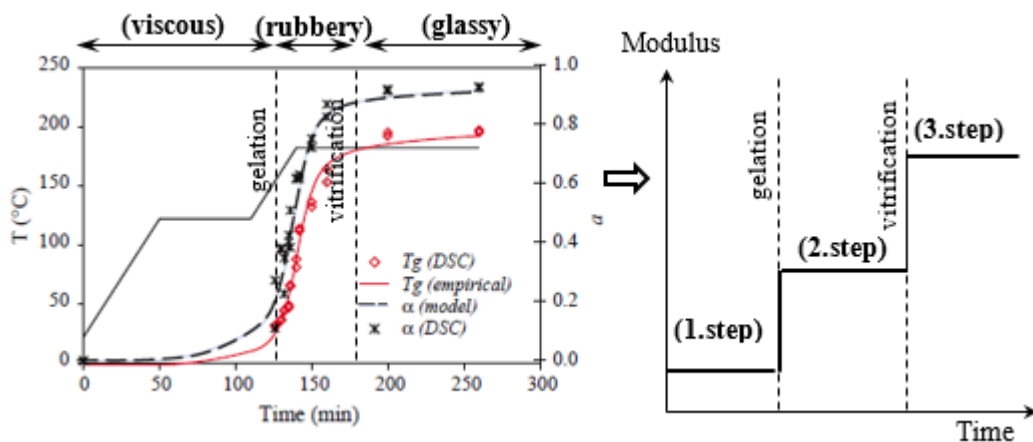

Figure 3. a)Various stages of the MRCC, b) Steps of FEM model

In the first step, before gelation, consolidation takes place as the voids are suppressed, expelled from the composite, and extra resin bleeds out in this step. Due to the difficulty in measuring the mechanical properties in the viscous state, there is no reliable data available for this state in the literature. In order to investigate the effect of the shear modulus in the viscous state, a parametric study is carried out by taking the shear modulus as different fractions of the rubbery shear modulus.

In the second step, between gelation and vitrification, rubbery material properties were used. Due to cross-linking reactions, cure shrinkage takes place during the curing of thermosetting resins, which results in contraction in the through thickness direction.

In the last step, after vitrification, glassy material properties were used in the model. The resin vitrifies and transforms to the glassy state and the resin modulus increases to a magnitude of a few GPa. The stresses developed in the viscous and rubbery states are rearranged as the part is allowed to deform freely as it cools down to room temperature by removing the boundary conditions.

The properties of AS4/8552 composite in the rubbery and glassy states were found in previous work [75] and are shown in Table 3.1. Cure shrinkage and CTE of the composite in the fibre direction assumed to be zero in Table 3.1. Gelation occurs when the temperature reaches to 160°C during the second ramp and vitrification occurs at 45 min after the start of the second hold at 180°C [29,75]. The CTE value given in this table for glassy state is the nominal value, and actual values are calculated as a function of corner thickness. To obtain the experimentally measured 0.48% [81] transverse cure shrinkage in the rubbery state, an equivalent negative Coefficient Of Thermal Expansion is used as given in Table 2. In Step-1 and Step-2, an autoclave pressure of 0.7 MPa is applied on the bag surface of the part. In Step-3, the applied pressure is removed, the part is separated from the tool and spring-in and warpage develops. A uniform temperature was assigned to the parts because the temperature range measured across the thickness and in the plane of the part at eight stations was within a 3 °C band for even the thickest (16 plies) laminates.

Table 2. Material properties in the rubbery and the glassy state [29].

Property	Unit	Rubbery	Glassy
E_{11}	MPa	132200	135000
$E_{22} = E_{33}$	MPa	165	9500
$G_{12} = G_{13}$	MPa	44.3	4900
G_{23}	MPa	41.6	4900
$v_{12} = v_{13}$	-	0.346	0.3
v_{23}	-	0.982	0.45

α_{11}	$\square\square°¢$	-	0^{*}
$\alpha_{22} = \alpha_{33}$	$\square\square°¢$	-31.7	32.6
ε_{11}^{cure}	%	0^{*}	-
$\varepsilon_{22}^{cure} = \varepsilon_{33}^{cure}$	%	0.48	-

*Assumed to be zero

Meshing and Boundary Conditions

A convergence study was performed in order to find the optimum mesh size. CPU times and deformation at the tip of a laminate were compared between C3D8 and C3D20R elements for UD4R25 sample (4-ply L shaped unidirectional laminate) by changing the element size. According to mesh convergence all 3D analysis were done using C3D20R elements of 3x3 mm.

Material orientation for 4 ply cross-ply laminate (XP4) is shown in (Figure 4). For this stacking sequence the bottom and the upper plies are fibre dominated along 1 direction, whereas the plies between the bottom and upper ply are resin dominated along the 1 direction.
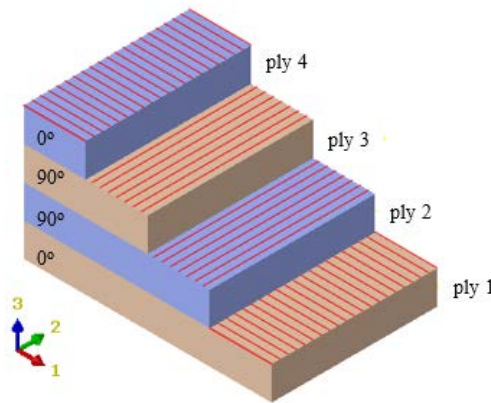

Figure 4. Material orientation used in ABAQUS for 4 -ply cross-ply laminate (XP4) with the designation of [0/90]$_s$

Flat strip parts are modelled with quarter of the full part by using symmetry boundary conditions. The symmetry planes and symmetry boundary conditions are shown in (Figure 5).
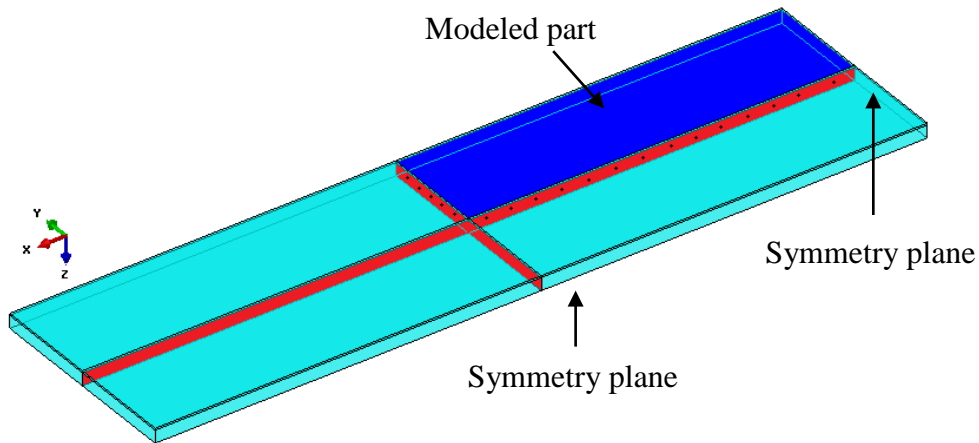
Figure 5. The symmetry planes and symmetry boundary conditions for flat strips parts

The sliding boundary conditions applied on the bottom surface of the tool that enables the tool to expand or contract along the in plane directions (x and y). The tool can extend or contract freely. Autoclave pressure is applied as a surface pressure on the upper surface of the laminate. Contact elements are used between the ply and the tool. The tool-part interaction to be sliding with constant shear stress and is assumed to be same for the two in-plane directions. Boundary conditions and applied autoclave pressure can be seen in (Figure 6).
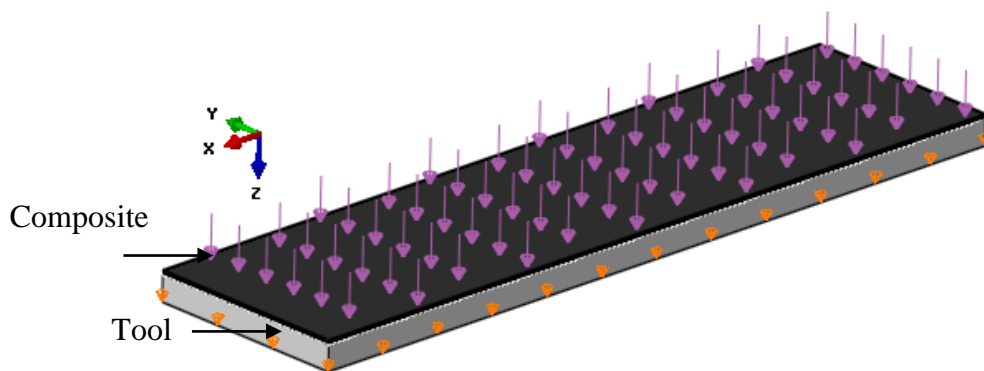

Figure 6. Loading and boundary conditions for flat strip parts.

Results and Discussion

The magnitude of warpage in unidirectional and cross-ply laminates was compared by changing the stacking sequence of the samples. It was observed that stacking sequence has a pronounced effect on distortion basically because of the effect of bending stiffness on warpage.

It was observed that unidirectional $[90]_4$ strip gives more warpage than cross-ply strips of $[0/90]_s$ and $[90/0]_s$ lay-up although both samples were subjected to the same tooling constraints. The reason behind this observation is as follows: tool-part

interaction effect is more pronounced for the [90]$_4$ samples due to stretching of fibres in 90 degree ply close to the tool. This generates more residual stress inside the laminate as compared to the other configurations. The warpage values are represented in (Figure 7).
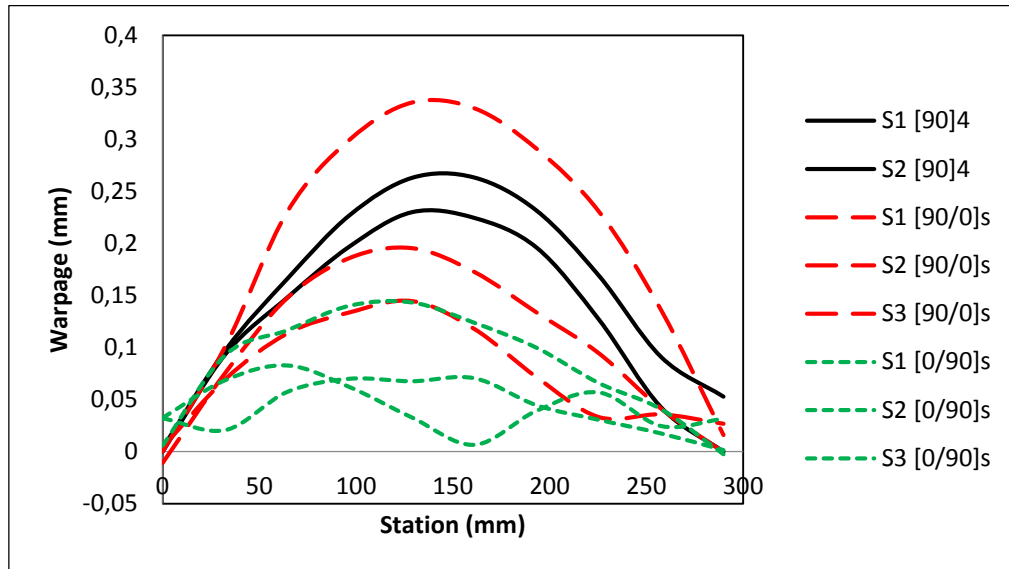

Figure 7. Warpage values for different stacking sequence

The warpage values were represented in (Figure 8). The solid continuous lines represented results of FEM and the dashed continuous lines represent the measured data. Three stacking sequences were modelled and manufactured: [90]$_4$,[0/90]$_s$, and [90/0]$_s$. Strips of [0]$_4$ were manufactured but warpage measurement could not be done due to lower bending stiffness so that FEM results were not added to the Figure 8. Predictions for the configuration of [90]$_4$ and [90/0]$_s$ strips are agree well with the measured data. On the other hand the model over predicted the warpage of [0/90]$_s$ strips.
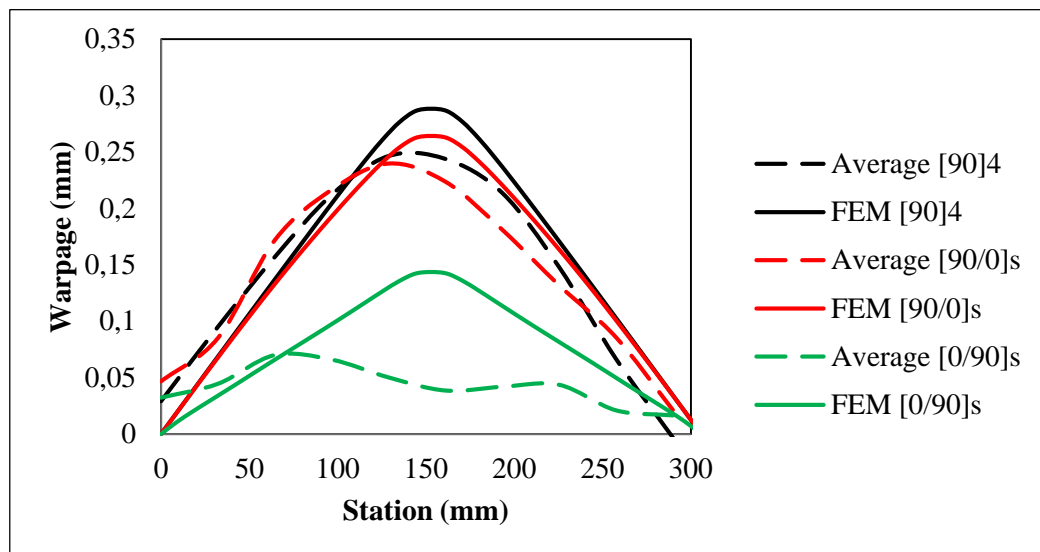

Figure 8. Spring-in predictions for flat strip parts of 300 mm length.

Conclusions

Fiber reinforced composite strips were manufactured and warpage values were measured and compared to the model results to investigate the model prediction capability. Also effect of stacking sequence on warpage was investigated. It was observed that unidirectional $[90]_4$ flat strip gives more warpage than cross-ply flat strips of $[0/90]_s$ and $[90/0]_s$ lay-up although both samples were subjected to the same tooling constraints. The reason behind this observation is as follows: tool-part interaction effect is more pronounced for the $[90]_4$ samples due to stretching of fibres in 90 degree ply close to the tool. This generates more residual stress inside the laminate as compared to the other configurations.

References

White, S.R., and Hahn, H.T., (1992). Process Modelling of Composite Materials: Residual Stress Development during Cure. Part I. Model Formulation. *Journal of Composite Materials*, 26(16), 2402-2422.

Bogetti, T.A., and Gillespie, J.W., (1992). Process-induced Stress and Deformation in Thick-section Thermoset Composite Laminates. *Journal of Composite Materials,* 26(5), 626-660.

Johnston, A., Vaziri, R., and Poursartip, A., (2001). A Plane Strain Model for Process-induced Deformation of Laminated Composite Structures", *Journal of Composite Materials,* 35(16), 1435-1469.

Svanberg, J.M., and Holmberg, J.A., (2001). An Experimental Investigation on Mechanisms for Manufacturing Induced Shape Distortions in Homogeneous and Balanced Laminates, *Composites Part A*, 32, 827–838.

Svanberg, J.M., Altkvist, C., and Nyman, T., (2005). Prediction of Shape Distortions for a Curved Composite C-spar, *Journal of Reinforced Plastics and Composites*, 24, 323.

Svanberg, J.M., and Holmberg, J. A., (2004). Prediction of Shape Distortions. Part II. Experimental Validation and Analysis of Boundary Conditions, *Composites: Part A* ,35, 723-734.

Ersoy, N., Garstka, T., Potter, K., and Wisnom, M.R., Porter, D., and Stringer, G., (2010). Modelling of the Spring-in Phenomenon in Curved Parts Made of a Thermosetting Composite, *Composite Part A*, 41, 410-418.

Ersoy, N., Garstka T., Potter K., Wisnom M.R., Porter D., Clegg M., et al. (2010). Development of the properties of a carbon fibre reinforced thermosetting composite through cure. *Composites: Part A*, 41, 401–409.

Wisnom, M.R., Ersoy. N., and Potter. K.D., (2007). Shear-lag analysis of the effect of thickness on spring-in of curved composites. *Journal of Composite Materials*, 41(11) ,1311–1324.

HexPly 8552 Epoxy matrix, Product Data, Hexcel Composites.